Journal of Organometallic Chemistry 694 (2009) 4223–4229

Contents lists available at ScienceDirect

Journal of Organometallic Chemistry

journal homepage: www.elsevier.com/locate/jorganchem

Opening "Jaws": Functionalisation of the hexaphosphapentaprismane cage, $P_6C_4{}^tBu_4$, affording $X_2P_6C_4{}^tBu_4$ (X = Me, I), crystal and molecular structures of $X_2P_6C_4{}^tBu_4$ (X = Me, I) and [*cis*-$PtCl_2Me_2P_6C_4{}^tBu_4$]

Mahmoud M. Al-Ktaifani, Martyn P. Coles, Ian R. Crossley, Lloyd T.J. Evans, Peter B. Hitchcock, Gerard A. Lawless *, John F. Nixon *

Chemistry Department, School of Life Sciences, University of Sussex, Brighton BN1 9QJ, Sussex, UK

ARTICLE INFO

Article history:
Received 21 July 2009
Accepted 1 September 2009
Available online 6 September 2009

Keywords:
Hexaphosphapentaprismane
Cage
Complex
Functionalisation

ABSTRACT

The hexaphosphapentaprismane cage, $P_6C_4{}^tBu_4$ ("Jaws"), can be readily opened by reaction with iodine at room temperature to afford the di-iodo derivative $I_2P_6C_4{}^tBu_4$ which can be converted to the dimethyl derivative $Me_2P_6C_4{}^tBu_4$ by treatment with LiMe. $Me_2P_6C_4{}^tBu_4$ behaves as a bidentate ligand towards $PtCl_2$. The molecular structures of all the new compounds have been determined by ^{31}P and/or ^{195}Pt NMR spectroscopy and single crystal X-ray diffraction studies.

1. Introduction

There is considerable current interest in P–C cage compounds in which phosphorus atoms are combined with isolobally related CR fragments containing bulky organic R groups; the two major synthetic routes involving oxidative coupling of the polyphospholyl anions $P_nC_{5-n}R_{5-n}$ ($n = 2, 3$) and thermal or metal-mediated oligomerisation of phosphaalkynes, P≡CR, (R = Bu^t Ad) [1,2]. A recent exciting development has been the synthesis of chiral cage compounds of the P_5-deltacyclene type and removal of the chiral auxiliary [3].

We and others have previously described a number of synthetic routes to the novel hexaphosphapentaprismane cage $P_6C_4{}^tBu_4$ **1** [2(m)]. Subsequently we reported a more convenient synthetic route involving ambient temperature oxidative coupling of two $P_3C_2{}^tBu_2$ anions by I_2 [2(o)].

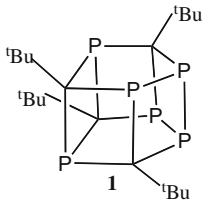

The hexaphosphapentaprismane cage **1** is unusual in that it readily undergoes a variety of ambient temperature insertion reactions *specifically and quantitatively* into the *unique* P–P bond linking the two 5-membered rings [4,5]. Thus, treatment with the chalcogens, E, (E = S, Se or Te), readily afforded the new cages shown in Scheme 1. The generality of this type of specific insertion was later confirmed by the reaction of **1** with a variety of other *isolobal* "heavy carbene-like" species, typified by the germylene GeR_2, stannylene SnR_2 and plumbylene, $PbAr_2$ [7] (Scheme 1).

An understanding as to why the *unique* P–P bond of **1** is the most reactive site in **1**, came from quantum chemical calculations carried out at the B3LYP/6-316G* level of theory on the hypothetical parent hexaphosphapentaprismane, $P_6C_4H_4$ [4], which revealed that both the HOMO and LUMO of the cage were concentrated at this particular P–P bond. In view of the ease and specificity of these insertion reactions we have likened this behaviour to that of the well-known shark "Jaws" of movie fame [4,5]. Also noteworthy is the *quantitative* insertion into **1** of the isolobal zerovalent platinum fragment [$Pt(PPh_3)_2$], even though there are no fewer than six phosphorus lone pairs available for simple σ-complexation to the metal [6] (Scheme 1). Likewise no simple η^1-ligated complex is detected (Scheme 2) in similar reactions of **1** with the Pt(II) centres in complexes [{$PtCl_2(PMe_3)$}$_2$] and [$PtCl_2(\eta^4$-COD)], where unexpectedly both insertion and chloride transfer reactions from Pt to P occurred [6] (Scheme 2).

To date, only one example has been reported of simple sigma coordination of **1** in the case of the Lewis acid AlI_3 [8]. We now

* Corresponding authors.
E-mail address: J.Nixon@sussex.ac.uk (J.F. Nixon).

0022-328X/$ - see front matter © 2009 Elsevier B.V. All rights reserved.
doi:10.1016/j.jorganchem.2009.09.002

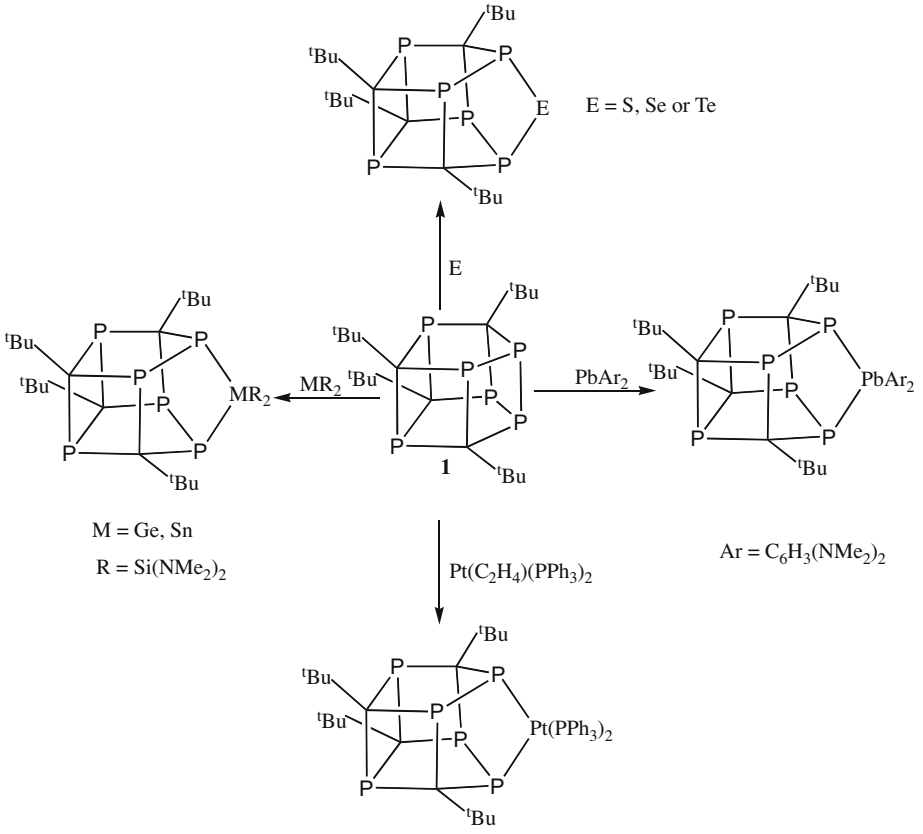

Scheme 1. Specific insertion reactions of S, Se, Te, MR_2 (M = Ge, Sn or Pb) and $Pt(PPh_3)_2$ into the unique P–P bond of **1**.

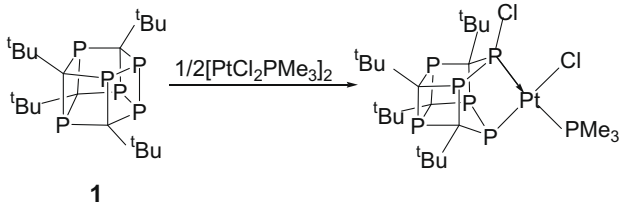

Scheme 2. Reaction of **1** with $[\{PtCl_2(PMe_3)\}_2]$ involves both insertion and chloride migration reaction from Pt to P.

describe experiments aimed at opening and thereby functionalising the hexaphosphapentaprismane cage $P_6C_4{}^tBu_4$ to generate compounds $X_2P_6C_4{}^tBu_4$ (X = I, Me) in which the unique P–P bond has been cleaved to form a more open structure containing two new P–X bonds. First results on the coordination of these new structures to platinum(II) are also presented and discussed.

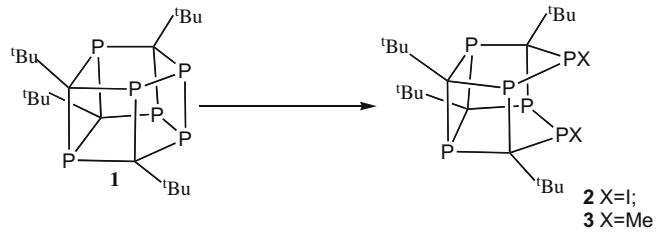

2. Results and discussion

Treatment of an equimolar amount of **1** with iodine in hexane or THF at room temperature gave **2** as a dark red crystalline compound. The $^{31}P\{^1H\}$ NMR spectrum exhibits the expected complex pattern of lines for the three types of phosphorus atoms reflecting the AA′MM′XX′ spin system, the resonances centred at 198.8, 140.7 and 116.8 ppm. Assignment of these resonances was made with recourse to our previous work with similar cages, such that the higher frequency resonance is attributed to P_C, that at 140.0 ppm to P_B and the lower frequency to P_A.

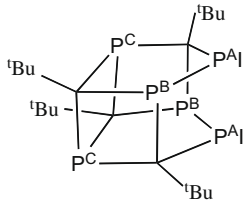

The molecular structure of **2** was confirmed by a single crystal X-ray analysis and is shown in Fig. 1.

The di-iodo compound can be readily converted into its dimethyl analogue $Me_2P_6C_4{}^tBu_4$ **3** on treatment with LiMe. The isolated product is a pale yellow crystalline solid, principally characterised by NMR spectroscopy. The replacement of the iodo groups by methyl substituents is implied by the ^1H NMR spectrum, which indicates the presence of a single methyl environment (δ_H 0.93), integrating as 6:18:18 against the two sets of ^tBu resonances. The multiplicity of the methyl resonance is basically doublet of doublet of doublets, due to coupling to the three distinct phosphorus environments, but exhibits some second order character inherent from the aforementioned magnetic inequivalences.

As with the parent di-iodo compound **2**, the $^{31}P\{^1H\}$ NMR spectrum of **3** exhibits three characteristic second order multiplets, but

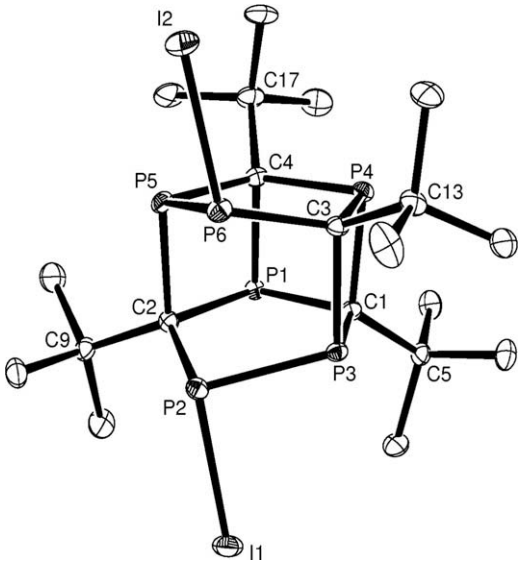

Fig. 1. Molecular structure of $I_2P_6C_4{}^tBu_4$ **2** (H-atoms omitted). Selected bond lengths (Å) and angles (°): P(2)–I(1) 2.5061(15), P(6)–I(2) 2.4930(15), P(3)–C(3) 1.926(5), P(4)–C(4) 1.874(6), P(4)–C(3) 1.885(6), P(4)–C(1) 1.908(5), P(5)–C(4) 1.884(6), P(5)–C(2) 1.936(5), P(5)–P(6) 2.194(2), P(6)–C(3) 1.866(6). C(1)–P(1)–C(2) 102.2(2), C(1)–P(1)–C(4) 85.6(2), C(2)–P(1)–C(4) 88.9(2), C(2)–P(2)–P(3) 98.35(17), C(2)–P(2)–I(1) 110.12(17), P(3)–P(2)–I(1) 93.66(6), C(1)–P(3)–C(3) 88.2(2), C(1)–P(3)–P(2) 101.73(17), C(3)–P(3)–P(2) 103.85(18), C(4)–P(4)–C(3) 102.1(2), C(4)–P(4)–C(1) 85.7(2), C(3)–P(4)–C(1) 88.5(2), C(4)–P(5)–C(2) 88.2(2), C(4)–P(5)–P(6) 102.42(18), C(2)–P(5)–P(6) 103.31(17), C(3)–P(6)–P(5) 98.17(18), C(3)–P(6)–I(2) 113.15(18), P(5)–P(6)–I(2) 94.12(7), C(5)–C(1)–P(1) 114.2(4), C(5)–C(1)–P(3) 116.8(4), P(1)–C(1)–P(3) 115.5(3), C(5)–C(1)–P(4) 120.8(4), P(1)–C(1)–P(4) 93.9(2), P(3)–C(1)–P(4) 91.8(2), C(9)–C(2)–P(2) 114.7(4), C(9)–C(2)–P(1) 115.8(4), P(2)–C(2)–P(1) 117.5(3), C(9)–C(2)–P(5) 111.8(4), P(2)–C(2)–P(5) 102.2(3), P(1)–C(2)–P(5) 91.0(2), C(13)–C(3)–P(6) 114.8(4), C(13)–C(3)–P(4) 115.0(4), P(6)–C(3)–P(4) 117.9(3), C(13)–C(3)–P(3) 112.8(4), P(6)–C(3)–P(3) 101.6(3), P(4)–C(3)–P(3) 91.0(2), C(17)–C(4)–P(4) 113.5(4), C(17)–C(4)–P(5) 117.3(4), P(4)–C(4)–P(5) 115.2(3), C(17)–C(4)–P(1) 121.9(4), P(4)–C(4)–P(1) 93.7(2), P(5)–C(4)–P(1) 91.6(2).

each shifted to significantly lower frequency (δ_P 182.3, 110.3 and 12.2). This shift is most apparent for the lower frequency resonance, which is thus assigned to the derivatised (P_A) centre, the resonances at 110 and 182 ppm being attributed to P_B and P_C, respectively.

In an effort to extract meaningful spin-spin coupling data, the $^{31}P\{^1H\}$ NMR spectrum of **3** was simulated [9]. The simulation output is shown in Fig. 2 alongside the experimentally observed spectra, and coupling constants are tabulated in Table 1.

The simulation affords a fair approximation of the experimental data, though it is noted that each resonance of the observed spectrum exhibits a different intrinsic line width, a factor not readily accommodated within the simulation, and the source of disparity. Though some caution must necessarily be applied to discussion of the extracted coupling constants, the patterns are clearly dominated by $|^1J_{AB}| = 195.7$ Hz, and $|^2J_{AB'}| = 76.5$ Hz, which prescribe the major features of the P_A and P_B resonances, respectively. The magnitude of $|J_{AC}|$ appears surprisingly small (8.2 Hz), but is a result of the sum of the contributions of two mediation pathways ($^2J + {}^3J$), in which the respective coupling constants are of opposite sign. Summative values are obtained for the remaining scalar interactions; the assignment of the J_{BC} coupling constant being based upon the presence of ^2J and ^3J pathways (opposite sign), *cf.* $J_{CB'}$ for which two ^2J pathways operate (same sign).

In all preparations of **3** the $^{31}P\{^1H\}$ NMR spectrum indicates the presence of trace amounts of a second material, characterised by several poorly resolved resonances. Although this species could not be separated or fully characterised, the lack of perturbation to the bulk elemental composition, together with the observed chemical behaviour (*vide infra*) leads us to tentatively assign it as the *endo–exo* conformational isomer of **3**.

Table 1
Simulated $^{31}P–^{31}P$ coupling constants for **3**, signs are relative.

J	Hz	J	Hz	J	Hz
$J_{AA'}$	1.1	$J_{BA'}$	76.5	$J_{CA'}$	−13.6
J_{AB}	195.7	$J_{BB'}$	0.46	$J_{CB'}$	−19.5
J_{AC}	−8.2	J_{BC}	2.2	$J_{CC'}$	−9.8

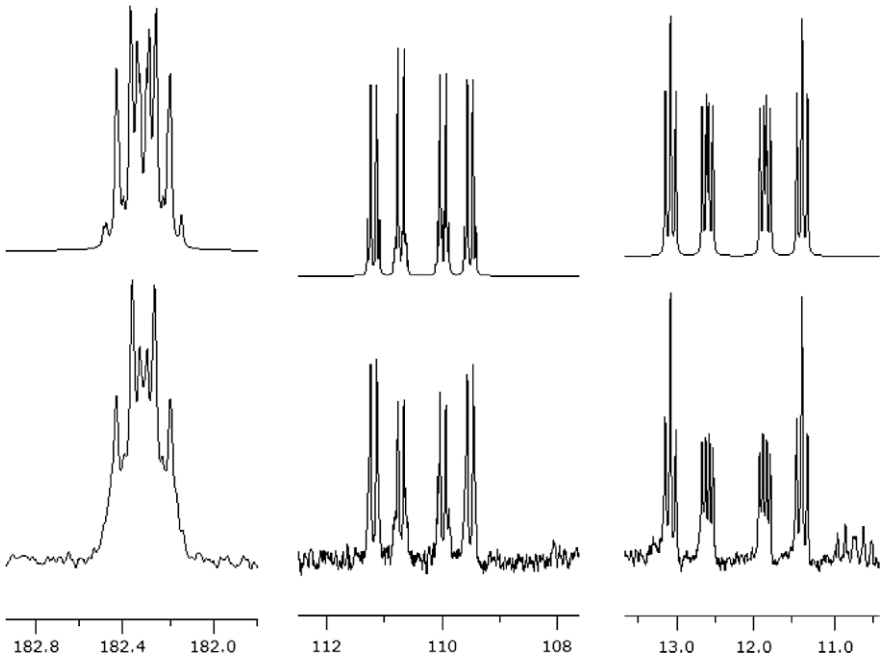

Fig. 2. Simulated (top) and observed (bottom) $^{31}P\{^1H\}$ NMR resonances for **3**. The RMS deviation between observed and calculated resonances is 0.015 Hz. The simulation has fixed line widths of 2 Hz.

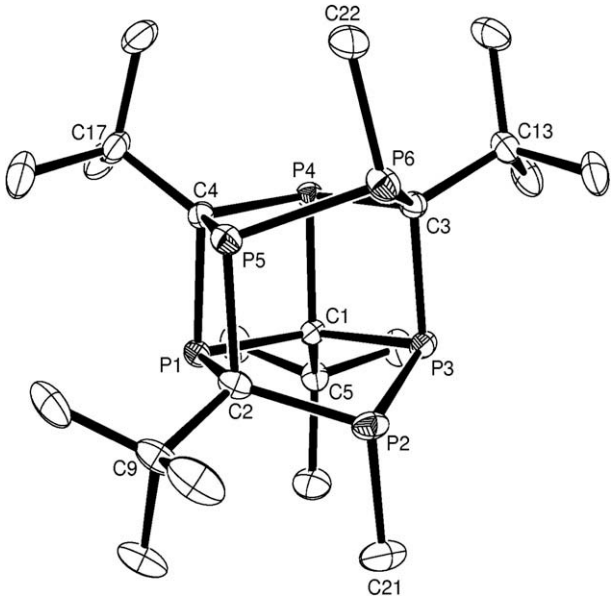

Fig. 3. Molecular structure of $Me_2P_6C_4{}^tBu_4$ **3** (H-atoms omitted). Selected bond lengths (Å) and angles (°): P(2)–C(2) 1.880(3), P(2)–C(21) 1.856(3), P(2)–P(3) 2.1739(11), P(3)–C(1) 1.882(3), P(3)–C(3) 1.910(3), P(4)–C(4) 1.880(3), P(4)–C(3) 1.891(3), P(4)–C(1) 1.905(3), P(5)–C(4) 1.888(3), P(5)–C(2) 1.908(3), P(5)–P(6) 2.1829(11), P(6)–C(22) 1.843(3), P(6)–C(3) 1.880(3). C(1)–P(1)–C(2) 102.42(12), C(1)–P(1)–C(4) 86.07(12), C(2)–P(1)–C(4) 88.23(12), C(21)–P(2)–C(2) 108.88(16), C(21)–P(2)–P(3) 95.77(13), C(2)–P(2)–P(3) 98.22(9), C(1)–P(3)–C(3) 88.19(12), C(1)–P(3)–P(2) 101.96(9), C(3)–P(3)–P(2) 105.11(9), C(4)–P(4)–C(3) 102.41(12), C(4)–P(4)–C(1) 85.81(12), C(3)–P(4)–C(1) 88.09(12), C(4)–P(5)–C(2) 88.15(12), C(4)–P(5)–P(6) 101.33(9), C(2)–P(5)–P(6) 105.84(10), C(22)–P(6)–C(3) 108.39(15), C(22)–P(6)–P(5) 94.77(12), C(3)–P(6)–P(5) 98.23(9), C(5)–C(1)–P(1) 113.59(18), C(5)–C(1)–P(3) 117.62(19), P(1)–C(1)–P(3) 114.69(14), C(5)–C(1)–P(4) 121.67(19), P(1)–C(1)–P(4) 93.71(12), P(3)–C(1)–P(4) 91.82(12), C(9)–C(2)–P(2) 113.7(2), C(9)–C(2)–P(1) 114.1(2), P(2)–C(2)–P(1) 115.29(15), C(9)–C(2)–P(5) 112.4(2), P(2)–C(2)–P(5) 107.62(14), P(1)–C(2)–P(5) 91.39(13), C(13)–C(3)–P(6) 113.58(19), C(13)–C(3)–P(4) 114.50(19), P(6)–C(3)–P(4) 114.94(14), C(13)–C(3)–P(3) 111.63(19), P(6)–C(3)–P(3) 108.56(14), P(4)–C(3)–P(3) 91.37(12), C(17)–C(4)–P(4) 113.7(2), C(17)–C(4)–P(5) 118.61(19), P(4)–C(4)–P(5) 114.67(14), C(17)–C(4)–P(1) 120.3(2), P(4)–C(4)–P(1) 93.63(12), P(5)–C(4)–P(1) 91.71(12).

The molecular structure of **3** was confirmed by a single crystal X-ray diffraction study and is shown in Fig. 3.

3. Coordination chemistry of 3

The geometry of **3** unsurprisingly renders it an effective bidentate ligand. Thus, upon treatment with one equivalent of $[PtCl_2(NCPh)_2]$, PhCN is displaced to afford, after removal of volatiles, a single phosphorus-containing product, formulated as [*cis*-$PtCl_2\{\kappa^2$-*P,P*-$Me_2P_6C_4{}^tBu_4\}$] **4** (Scheme 3). Recrystallisation from dichloromethane (−45 °C) affords **4** as colourless crystals that were subject to comprehensive multinuclear NMR spectroscopic and single crystal X-ray diffraction studies (*vide infra*).

The $^{31}P\{^1H\}$ NMR spectrum of **4** again exhibits a characteristic AA′MM′XX′ pattern (76.2, 92.5 and 169.9 ppm), the two lower frequency resonances exhibiting platinum satellite coupling (^{195}Pt, I = ½, 33.3%); (Fig. 4). The relative magnitudes of J_{PtP} enable unequivocal assignment of the three resonances, the lower frequency being assigned to the chelating *PMe* centres, while the highest frequency resonance, for which platinum satellites are lost within the signal envelope, is assigned to the rear face of the tetraphospha-cubane core. The magnitude of J_{PtP} for the chelating centre (3162 Hz) of **4** is consistent with the anticipated *cis*-geometry.

These conclusions are reflected by the $^{195}Pt\{^1H\}$ NMR spectrum, (Fig. 5) which exhibits a single resonance, centred at −4068 ppm, split as a triplet of triplet of triplets (Fig. 5), indicating coupling to all three sets of ^{31}P nuclei (J_{PtPA} 3165, J_{PtPB} 204, J_{PtPC} 57 Hz),

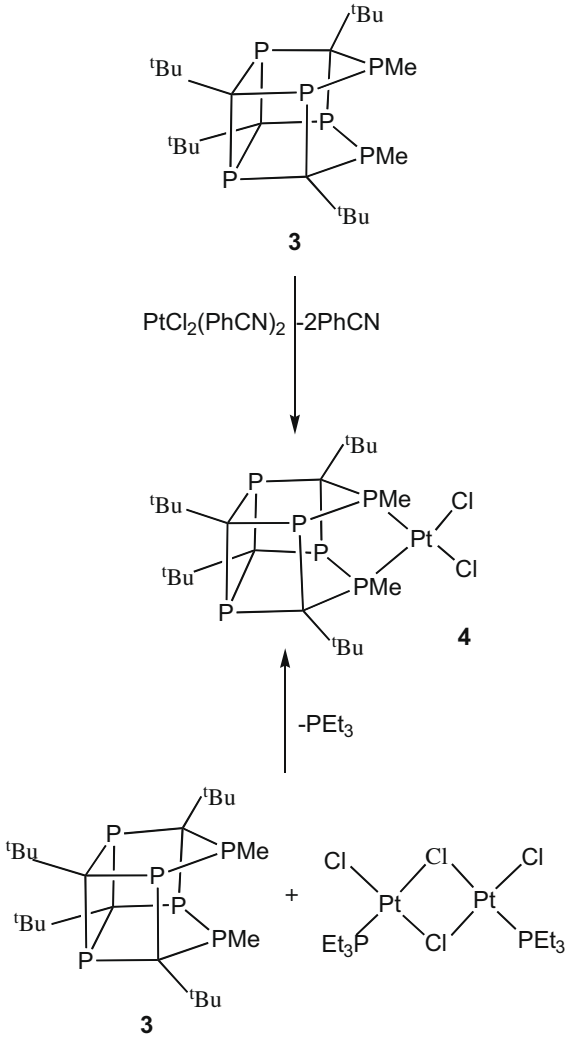

Scheme 3.

which with respect to platinum appear as a simple AMX spin system.

The molecular structure of **4** was confirmed by a single crystal X-ray diffraction study and is shown in Fig. 6.

Given the presence of an apparently second conformational isomer in all samples of **3** (*vide supra*) and the multitude of potential coordination sites within the $Me_2P_6C_4{}^tBu$ cage, the possibility for monodentate coordination to one of more metal centres was briefly explored. To this end, **3** was treated with one equivalent of $[PtCl_2(PEt_3)]_2$, affording a colourless, microcrystalline product. However, monitoring of the reaction products by NMR spectroscopy revealed only 50% consumption of the platinum dimer, with formation, once again, of the chelate complex **4**, the result of bridge-cleavage and concomitant displacement of the PEt_3 ligand. This reaction was not pursued further, but serves to illustrate the potency of **3** as a chelating ligand, apparently to the exclusion of all other coordination modes. Indeed, it would seem the propensity to chelate may even induce conformational change.

4. Experimental

4.1. General procedures

All the air and moisture sensitive compounds were manipulated under an atmosphere of high purity argon using conventional

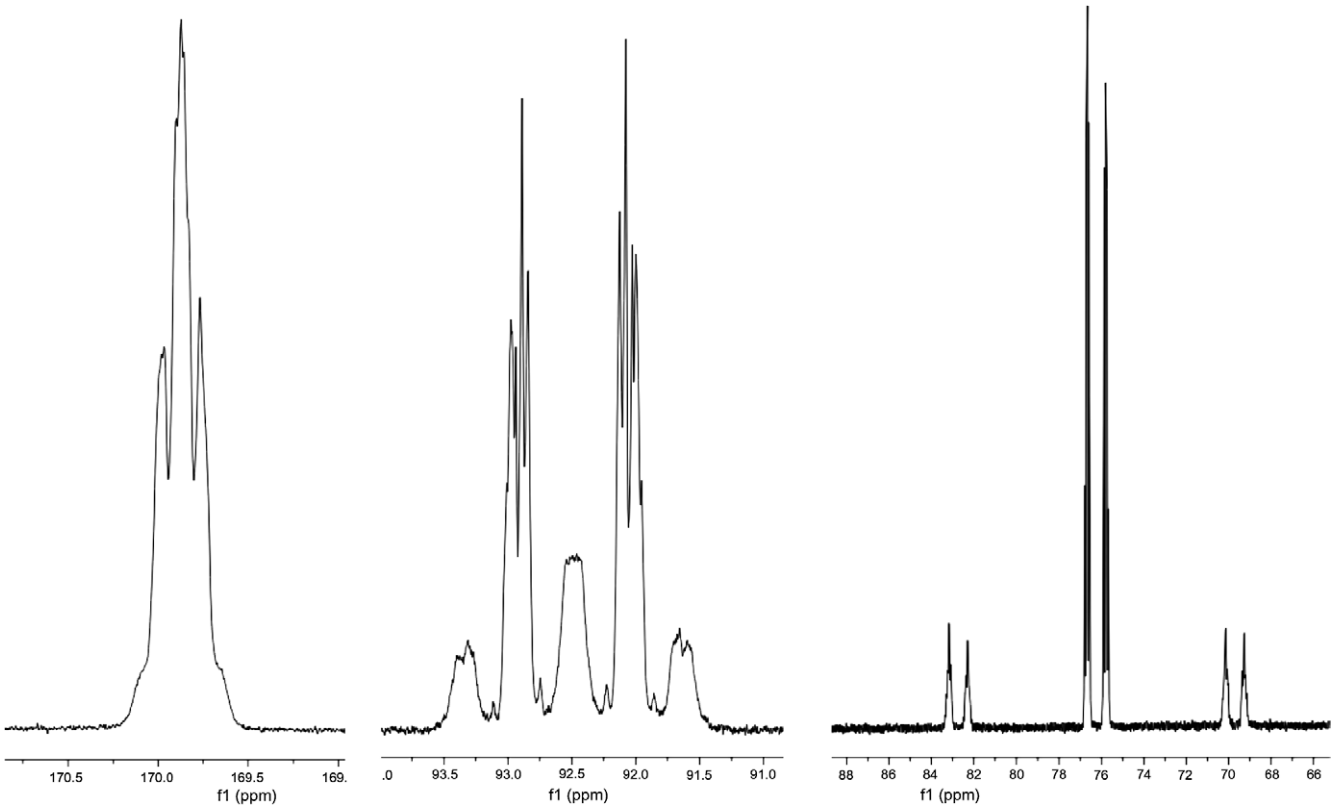

Fig. 4. $^{31}P\{^{1}H\}$ NMR spectrum of **4**.

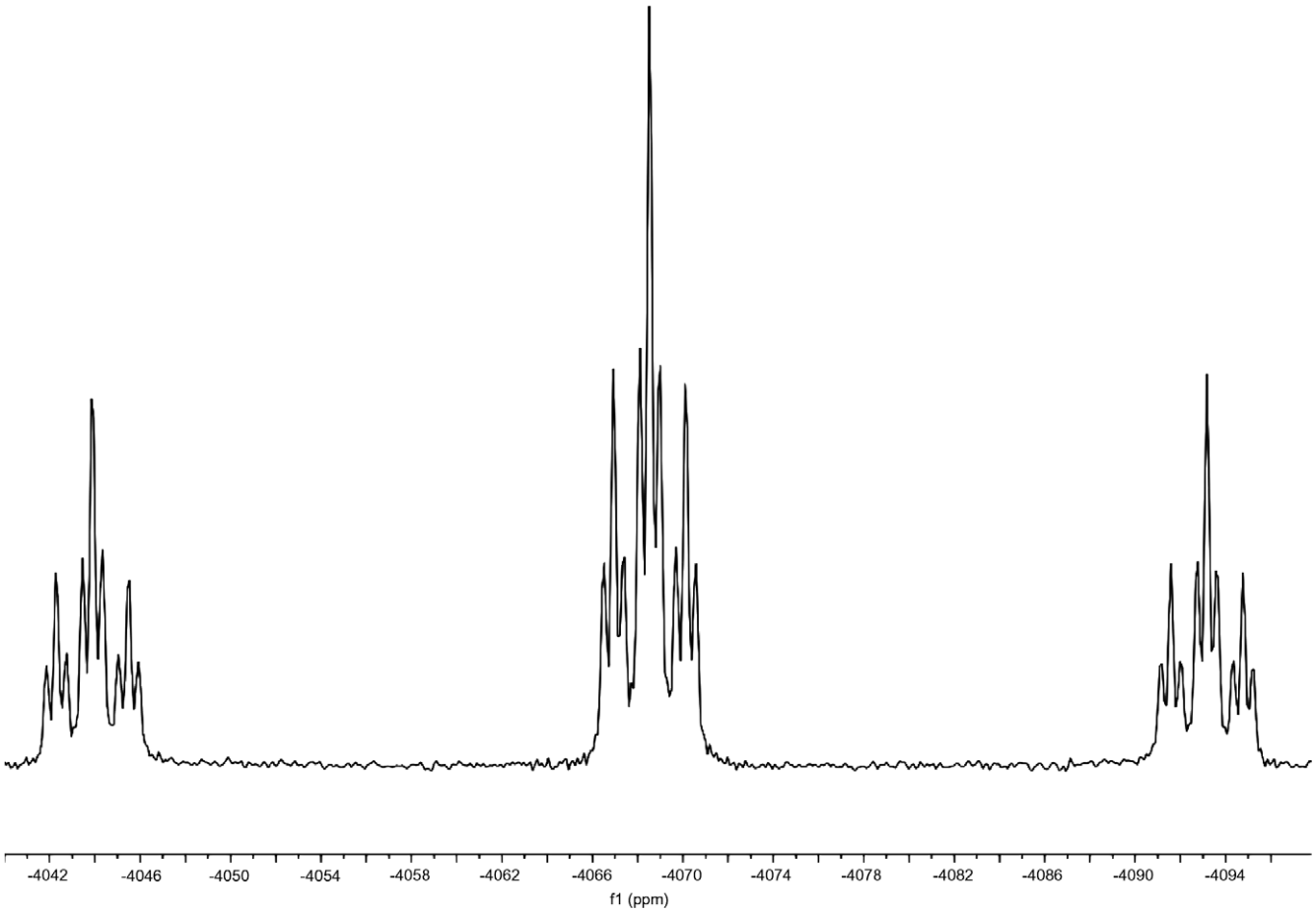

Fig. 5. $^{195}Pt\{^{1}H\}$ NMR spectrum of **4**.

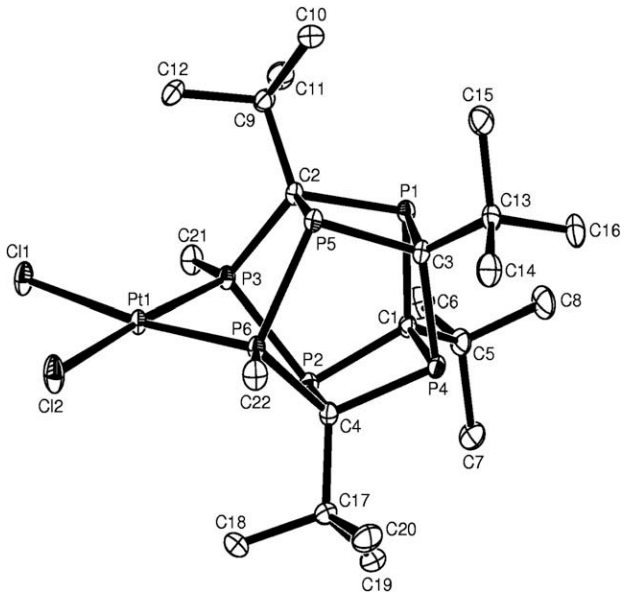

Fig. 6. Molecular structure of $[PtCl_2Me_2P_6C_4{}^tBu_4]$ **4** (H-atoms omitted). Selected bond lengths (Å) and angles (°): Pt(1)–P(6) 2.2190(7), Pt(1)–P(3) 2.2208(7), Pt(1)–Cl(2) 2.3467(7), Pt(1)–Cl(1) 2.3505(7), P(1)–C(1) 1.884(3), P(1)–C(2) 1.902(3), P(1)–C(3) 1.904(3), P(2)–C(1) 1.873(3), P(2)–C(4) 1.911(3), P(2)–P(3) 2.1768(10), P(3)–C(21) 1.815(3), P(3)–C(2) 1.854(3), P(4)–C(3) 1.884(3), P(4)–C(1) 1.904(3), P(4)–C(4) 1.909(3), P(5)–C(3) 1.875(3), P(5)–C(2) 1.907(3), P(5)–P(6) 2.1732(10), P(6)–C(22) 1.810(3), P(6)–C(4) 1.853(3). P(6)–Pt(1)–P(3) 79.43(2), P(6)–Pt(1)–Cl(2) 94.69(3), P(3)–Pt(1)–Cl(2) 174.11(3), P(6)–Pt(1)–Cl(1) 172.52(3), P(3)–Pt(1)–Cl(1) 94.56(2), Cl(2)–Pt(1)–Cl(1) 91.32(3), C(1)–P(1)–C(2) 102.37(12), C(1)–P(1)–C(3) 86.24(12), C(2)–P(1)–C(3) 88.01(11), C(1)–P(2)–C(4) 88.75(12), C(1)–P(2)–P(3) 99.85(9), C(4)–P(2)–P(3) 99.94(9), C(21)–P(3)–C(2) 114.81(13), C(21)–P(3)–P(2) 102.81(11), C(2)–P(3)–P(2) 102.04(9), C(21)–P(3)–Pt(1) 119.36(10), C(2)–P(3)–Pt(1) 111.01(8), P(2)–P(3)–Pt(1) 104.17(3), C(3)–P(4)–C(1) 86.25(12), C(3)–P(4)–C(4) 102.78(12), C(1)–P(4)–C(4) 87.89(11), C(3)–P(5)–C(2) 88.71(12), C(3)–P(5)–P(6) 99.91(9), C(2)–P(5)–P(6) 99.99(8), C(22)–P(6)–C(4) 113.92(14), C(22)–P(6)–P(5) 103.49(11), C(4)–P(6)–P(5) 102.45(9), C(22)–P(6)–Pt(1) 118.65(10), C(4)–P(6)–Pt(1) 114.14(9), P(5)–P(6)–Pt(1) 101.04(3).

Schlenk or glove box techniques. Solvents were meticulously dried and were distilled and freeze-thaw degassed before use. NMR spectra were recorded on Varian Direct Drive 400 (^{1}H 399.495 MHz, referenced to external $SiMe_4$; $^{31}P\{^1H\}$ 161.713 MHz, referenced to external 85% H_3PO_4) or 600 (^{1}H 599.689 MHz, referenced to external $SiMe_4$; $^{31}P\{^1H\}$ 242.799 MHz, referenced to external 85% H_3PO_4; $^{195}Pt\{^1H\}$ 128.397 MHz, referenced to external K_2PtCl_6) instruments. Microanalyses were carried out by Labor Pascher, Remagen, Germany. Single crystal X-ray structures were determined using a Nonius Kappa CCD diffractometer. All structures were refined using SHELXL-97.

Preparation of starting materials:

*4.1.1. Preparation of $P_6C_4{}^tBu_4$ **1***

A solution of $KP_3C_2Bu^t_2$ (2.0 g, 7.40 mmol) in THF (60 ml) was treated with a solution of I_2 (0.94 g, 3.70 mmol) in THF (30 ml) at ambient temperature, causing an immediate colour change to orange, with concomitant precipitation of KI. The reaction mixture was left stirring at ambient temperature for 12 h. Volatile components were then removed *in vacuo* and the solid residue was extracted with warm (approx. 40 °C) hexane (approx. 100 ml), and filtered, *via* cannula, to exclude insoluble KI. The hexane extract was concentrated *in vacuo* to approximately 20 ml, and cooled to −45 °C in a freezer overnight to give **1** as an orange crystalline solid. Isolated yield = 1.12 g, 65%.

*4.1.2. Preparation of $P_6C_4{}^tBu_4I_2$ **2***

A solution of I_2 (0.041 g, 0.163 mmol) in hexane (10 ml) was added to a solution of $P_6C_4{}^tBu_4$ (0.075 g, 0.163 mmol) in hexane (10 ml) at room temperature. The colour of the solution immediately changed to red. The solvent was then removed *in vacuo* to afford quantitatively $P_6C_4{}^tBu_4I_2$ as evidenced by $^{31}P\{^1H\}$ NMR spectroscopy. The product was further purified by crystallization from hexane at −30 °C to give $P_6C_4{}^tBu_4I_2$ as a red crystalline solid (0.33 g, 40%). Anal. Calc. for $C_{20}H_{36}P_6I_2$: C, 34.11; H, 5.35. Found: C, 33.54; H, 5.07%.

An improved yield was obtained using the following procedure: A solution of **1** (0.400 g, 0.87 mmol) in THF (60 ml) was treated with a solution of I_2 (0.220 g, 0.87 mmol) in THF (30 ml) at ambient temperature, causing an immediate colour change from orange to dark red. The solution was stirred for a further 60 min at ambient temperature. The volatile components were then removed *in vacuo*. The solid residue was extracted with hot (approx. 70 °C) heptane (approx. 80 ml), and filtered using a cannula to exclude a small quantity of insoluble material. The heptane extract was concentrated *in vacuo* to approximately 20 ml, and slow-cooled to −45 °C in a freezer overnight to give the product as a dark red crystalline solid. Isolated yield = 0.490 g, 79%.

*4.1.2.1. Spectroscopic data for **2**.* (C_7D_8, 25 °C), $^{31}P\{^1H\}$ NMR (161.72 MHz): δ_P = 116.8, δ_P = 140.7, δ_P = 198.8 see text. ^{1}H NMR (399.50 MHz): $\delta_H(^tBu)$ = 1.34 (s, 18H), $\delta_H(^tBu)$ = 1.41 (s, 18H). MS. (EI), *m*/*z*: 717 (55%, $[M]^+$), 589 (55%, $[M-I]^+$).

*4.1.2.2. Crystal data for **2**.* $C_{20}H_{36}I_2P_6$, M = 716.11, orthorhombic, space group *Pbca* (No. 61) a = 14.0608(1), b = 23.6999(3), c = 16.4024(2) Å; V = 5465.93(10) Å^3, T = 173(2) K, Z = 8, D_c = 1.74 Mg m^{-3}, μ = 2.66 mm^{-1}, λ = 0.71073 Å, F(0 0 0) = 2816, crystal size 0.15 × 0.10 × 0.05 mm^3, 54 755 measured reflections, 4798 independent reflections (R_{int} = 0.068), 4173 reflections with $I > 2\sigma(I)$, final indices R_1 = 0.044, wR_2 = 0.098 for $I > 2\sigma(I)$, R_1 = 0.053, wR_2 = 0.102 for all data. Data collection: KappaCCD. Program package WinGX. Refinement using SHELXL-97.

*4.1.3. Preparation of $P_6C_4{}^tBu_4Me_2$ **3***

A solution of **2** (0.250 g, 0.35 mmol) in diethyl ether (40 ml) was cooled to −78 °C and treated with methyllithium (2.30 ml of a 0.334 M solution in diethyl ether, 0.77 mmol). The solution was stirred for a further 60 min at −78 °C, during which time a colour change from dark red to pale yellow was observed. The solution was allowed to warm to ambient temperature, and the volatile components were then removed *in vacuo*. The solid residue was extracted with hexane (approx. 60 ml) and filtered *via* cannula to exclude insoluble LiI. The hexane extract was concentrated *in vacuo* to approximately 5 ml, and cooled to −45 °C in a freezer overnight to give the product as a light yellow crystalline solid. Isolated yield = 0.105 g, 61%.

See the text for a discussion of the NMR spectroscopic data.

*4.1.3.1. Crystal data for **3**.* $C_{22}H_{42}P_6$, M = 492.38, monoclinic, space group $P2_1/c$ (No. 14) a = 16.1749(3), b = 10.4089(2), c = 16.5597(4) Å, β = 107.550(1); V = 2658.27(10) Å^3, T = 173(2) K, Z = 4, D_c = 1.23 Mg m^{-3}, μ = 0.41 mm^{-1}, λ = 0.71073 Å, F(0 0 0) = 1056, crystal size 0.20 × 0.20 × 0.15 mm^3, 16 231 measured reflections, 4516 independent reflections (R_{int} = 0.069), 3770 reflections with $I > 2\sigma(I)$, final indices R_1 = 0.0440, wR_2 = 0.1040 for $I > 2\sigma(I)$, R_1 = 0.0564, wR_2 = 0.1109 for all data. Data collection: KappaCCD. Program package WinGX. Refinement using SHELXL-97.

*4.1.4. Preparation of $Me_2P_6C_4{}^tBu_4PtCl_2$ **4***

THF (30 ml) was added to a dry mixture of **3** (0.125 g, 0.254 mmol) and $PtCl_2(PhCN)_2$ (0.120 g, 0.254 mmol) at ambient temperature, yielding a clear, mostly colourless solution. The solution was allowed to stir for a further 12 h at ambient temperature. The volatile components were then removed *in vacuo*. The solid residue

was extracted with CH_2Cl_2 (approx. 30 ml) and filtered (filter cannula) to remove a small amount of black insoluble material, presumed to be elemental platinum. The CH_2Cl_2 extract was concentrated *in vacuo* to approximately 2 ml, and cooled to −45 °C in a freezer overnight to give the product as a colourless crystalline solid. Isolated yield = 0.116 g, 60%. See text for a discussion of the NMR spectra of **4**.

4.1.4.1. Crystal data for ***4****.* $2.5CH_2Cl_2$: $C_{22}H_{42}Cl_2P_6Pt$, $2.5(CH_2Cl_2)$ $M = 970.68$, triclinic, space group $P\bar{1}$ (No. 2), $a = 10.8158(1)$, $b = 13.0554(2)$, $c = 13.9320(3)$ Å, $\alpha = 96.277(1)°$, $\beta = 103.299(1)°$, $\gamma = 94.768°$; $V = 1891.07(5)$ Å^3, $T = 173(2)$ K, $Z = 2$, $D_c = 1.71$ Mg m^{-3}, $\mu = 4.48$ mm^{-1}, $\lambda = 0.71073$ Å, $F(0\,0\,0) = 962$, crystal size $0.25 \times 0.10 \times 0.08$ mm^3, 35 244 measured reflections, 8852 independent reflections ($R_{int} = 0.046$), 8217 reflections with $I > 2\sigma(I)$, final indices $R_1 = 0.025$, $wR_2 = 0.055$ for $I > 2\sigma(I)$, $R_1 = 0.028$, $wR_2 = 0.057$ for all data. Data collection: KappaCCD. Program package WinGX. Refinement using SHELXL-97.

Acknowledgements

We thank the EPSRC for their continuing financial support for phospha-organometallic chemistry at Sussex. I.R.C. also gratefully acknowledges the award of a Royal Society Research Fellowship. We thank Dr. I.J. Day for acquiring multinuclear NMR spectroscopic data.

Appendix A. Supplementary material

Supplementary data associated with this article can be found, in the online version, at doi:10.1016/j.jorganchem.2009.09.002.

References

[1] (a) K.B. Dillon, F. Mathey, J.F. Nixon, Phosphorus: The Carbon Copy: From Organophosphorus to Phospha-organic Chemistry, Wiley, 1998;
(b) F. Mathey (Ed.), Phosphorous–Carbon Heterocyclic Chemistry: The Rise of a New Domain, Pergamon, Oxford, 2001;
(c) F. Mathey, Angew. Chem., Int. Ed. 42 (2003) 1578.
[2] (a) R. Streubel, Angew. Chem., Int. Ed. 34 (1995) 436. and references therein;
(b) A. Mack, M. Regitz, in: K.K. Laali (Ed.), Carbocyclic and Heterocyclic Cage Compounds and Their Building Blocks, J.A.I. Press, Stamford, CT, USA, 1999, p. 199;
(c) J.F. Nixon, in: K.K. Laali (Ed.), Carbocyclic and Heterocyclic Cage Compounds and Their Building Blocks, J.A.I. Press, Stamford, CT, USA, 1999, p. 257;
(d) L. Weber, Adv. Organometal. Chem. 41 (1997) 1;
(e) M. Regitz, A. Hoffmann, U. Bergsträsser, in: P.J. Stang, F. Diederich (Eds.), Modern Acetylene Chemistry, VCH, Weinheim, 1995;
(f) R. Appel, in: M. Regitz, O. Scherer (Eds.), Multiple Bonds and Low Coordination in Phosphorus Chemistry, Georg Thieme Verlag, New York, 1990, p. 153;
(g) R. Bartsch, P.B. Hitchcock, J.F. Nixon, J. Organometal. Chem. 375 (1989) C31;
(h) V. Caliman, P.B. Hitchcock, J.F. Nixon, M. Hofmann, P. von R. Schleyer, Angew. Chem., Int. Ed. 33 (1994) 2202;
(i) B. Geissler, T. Wettling, S. Barth, P. Binger, M. Regitz, Synthesis (1994) 1337;
(j) F. Tabellion, A. Nachbauer, S. Leininger, C. Peters, F. Preuss, M. Regitz, Angew. Chem., Int. Ed. 37 (1998) 1233;
(k) T. Wettling, J. Schneider, O. Wagner, C.G. Kreiter, M. Regitz, Angew. Chem., Int. Ed. 28 (1989) 1013;
(l) B. Geissler, S. Barth, U. Bergsträsser, M. Slany, J. Durkin, P.B. Hitchcock, M. Hofmann, P. Binger, J.F. Nixon, P. von R. Schleyer, M. Regitz, Angew. Chem., Int. Ed. 34 (1995) 484;
(m) M.M. Al-Ktaifani, W. Bauer, U. Bergsträsser, B. Breit, M.D. Francis, F.W. Heinemann, P.B. Hitchcock, A. Mack, J.F. Nixon, H. Pritzkow, M. Regitz, M. Zeller, U. Zenneck, Chem. Eur. J. 8 (2002) 2622;
(n) A.G. Avent, F.G.N. Cloke, M.D. Francis, P.B. Hitchcock, J.F. Nixon, Chem. Commun. (2000) 879;
(o) M.M. Al-Ktaifani, P.B. Hitchcock, J.F. Nixon, Inorg. Chim. Acta 356 (2003) 103.
[3] M. Hofmann, C. Hohn, F.W. Heinemann, U. Zenneck, Chem. Eur. J. 15 (2009) 5998.
[4] M.M. Al-Ktaifani, D.P. Chapman, M.D. Francis, P.B. Hitchcock, J.F. Nixon, L. Nyulászi, Angew. Chem., Int. Ed. 40 (2001) 3474.
[5] "Jaws" Directed by Stephen Spielberg, Universal Pictures, 1975.
[6] M.M. Al-Ktaifani, P.B. Hitchcock, J.F. Nixon, J. Chem. Soc., Dalton. Trans. (2008) 1132.
[7] M.M. Al-Ktaifani, P.B. Hitchcock, M.F. Lappert, J.F. Nixon, P. Uiterweerd, J. Chem. Soc., Dalton Trans. (2008) 2825.
[8] M.M. Al-Ktaifani, P.B. Hitchcock, J.F. Nixon, J. Mol. Struct. 922 (2009) 109.
[9] K. Marat, Spinworks 3.0, University of Manitoba, 2008.